Preprints of the
9th International Symposium on Advanced Control of Chemical Processes
The International Federation of Automatic Control
June 7-10, 2015, Whistler, British Columbia, Canada

Economics-Oriented NMPC of Two-Stage-Riser Catalytic Pyrolysis Processes for Maximizing Propylene Yield

Ping Wang[a, b], Xuemin Tian[a], Chaohe Yang[b], Zhihong Yuan[c]

a. College of Information and Control Engineering, China University of Petroleum, Qingdao, 266580, China (Tel: +86-532-86983467; e-mail: wangpingupc@upc.edu.cn, tianxm@upc.edu.cn).

b. State Key Laboratory of Heavy Oil Processing, China University of Petroleum, Qingdao, 266580, China (e-mail: yangch@upc.edu.cn)

c. Department of Chemical Engineering, Auburn University, Auburn, AL36849, United States (e-mail: zzy0013@auburn.edu)

Abstract: Two-stage-riser fluidized catalytic pyrolysis for maximizing propylene yield (TMP) process focuses on propylene production meanwhile without significant losses on gasoline/diesel yields. The complex nonlinear behaviour of this process calls for advanced control system to tackle various disturbances to achieve optimal operation. This paper is devoted to presenting an economics-oriented NMPC scheme that could maximize propylene production while satisfying process operation constraints. In the proposed scheme, those variables, which are difficult to be measured online, including product yields as well as uncertain model parameters are estimated by an unscented transformation based Kalman filter. Potential economic benefits and robustness associated with the proposed controller scheme are illustrated through simulations.

Keywords: Catalytic pyrolysis, Two-stage-riser, Economic predictive control, State estimation

1. INTRODUCTION

Propylene is one of the most crucial building blocks mainly used in polymer and rubber industry. Commercial routes for propylene production are steam cracking of naphtha or liquid petroleum gas (LPG) as well as fluid catalytic cracking (FCC) of heavy hydrocarbon liquids. Currently, high growth rate of propylene demand combined with the declined quantity of propylene from steam cracking processes, are expanding the demand/supply gap of propylene and in turn enhance its price. Consequently, a wide variety of novel FCC processes have emerged to cope with the evolving needs of the propylene market. Among these processes, the two-stage-riser catalytic pyrolysis for maximizing propylene yield (TMP) process, which applies a subsidiary riser operated under appropriate condition to reprocess gasoline from the main riser fed with fresh feedstock, represents an attractive alternative for propylene production while maintaining relatively high yield of gasoline (Li *et al*. 2007).

Facing changeable industrial environment, TMP plants need to process various feedstocks with different qualities to meet market demands, the overall economic benefits of this process can be considerably enhanced if proper optimization and control strategies are implemented. However, because of the strong interactions among two risers and the regenerator along with the constraints for the safe and stable operation, designing an efficient control system for TMP process is challenging. Over the past two decades, model predictive control (MPC), which deals with the control problem through transforming it into an optimization problem, has emerged as a promising approach for tackling complex control problems for large-scale industrial processes (Qin & Badgwell.2003). The classical objective function of MPC is a quadratic index which penalizes the deviations of the outputs and inputs from the targets. Recently, the development of MPC with a general economic cost function has been studied extensively (Engell, 2007. Ellis *et al*, 2014). This scheme, known as economic model predictive control (EMPC), seems to be ideally suited for addressing the optimization and control problems associated with operation of TMP processes. In this work, an EMPC formulation based on previous experience for control of FCC process (Zanin *et al*. 2002) is developed for the TMP process. Here, it is necessary to highlight the differences and similarities between TMP and FCC processes along with their respective control problems. Conventional FCC units has only one single riser reactor to convert heavy oil fractions into a wide range of products of which gasoline is the most valuable. On the other hand, TMP technology is specifically focusing on maximizing propylene production through combining the effects of ZSM-5 catalyst additive and the second high severity riser to selectively crack olefins in the gasoline range to propylene. Clearly, changes in products of the first riser can alter the composition and property of the feedstock for the second riser and thus affect the whole reaction systems. This invites to extend control techniques and ideas proven successful for the FCC process to the TMP process as proposed in this paper.

Based on a pilot-scale unit, a first-principle dynamic model, which takes into account kinetics of pyrolysis reactions in two risers and kinetics of coke combustion in regenerator, has been derived for TMP process. In this paper, an economics-oriented nonlinear MPC scheme is used to formulate the optimization and control of TMP process as a dynamic optimization problem. An unscented trans-formation based Kalman filter is proposed to realize the online-estimate of unmeasured product yields and uncertain model parameters. Potential economic benefits of the proposed method are elucidated by means of simulations, i.e. maximizing the productivity of propylene following the experimental condition reported by (Li *et al*. 2007) and robustness with respect to variations in model parameters.

2. PROCESS DESCRIPTION

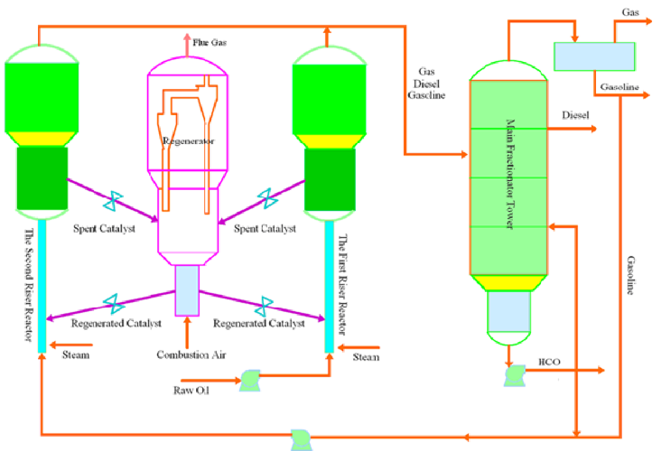

Fig. 1. Schematic of the TMP riser reactor unit.

Fig.1 shows a typical TMP flow sheet, which contains two riser reactors and a regenerator. TMP process is developed based on the two-stage reactor FCC (TSRFCC) technology (Shan *et al*. 2001). The cracking reaction of the hydrocarbon feedstock takes place in two risers, whereas the regenerator reactivates catalyst by burning coke deposited on them. The first riser deals with atmospheric residue, whereas the second stage is fed with recycle oil and light gasoline, both coming from the first riser. The feed is subsequently vaporized when it contacts with hot catalyst particles from the regenerator. Endothermic catalytic pyrolysis reactions generate lighter hydrocarbons as the main cracking products along with coke as by-product that deposits on the catalyst surface which hence reduces the activity of catalyst. The regenerator is attached with a high-efficiency combustor and an external catalyst cooler. The combustor, where the gas and the solid flows are fast-fluidized with the excess air, ensures a very low level of coke content of regenerated catalyst. The cooler helps to remove superfluous heat that exceeds the requirement for heat balance and thus to control regenerator temperature within a desired range.

3. PROCESS MODELING

This section presents an integrated mathematical model that allows the prediction of the dynamic behaviour and the product distributions of TMP process. The reaction mechanism in each risers is described as the 11-lump kinetic model, as **Table 1** presented. The corresponding kinetic parameters can be found in (Guo.2008). It is assumed that all of the feed oil is completely vaporized at the feed inlet. Due to the short residence time of oil vapour in two risers (1.1s~1.5s), two risers are assumed to be modelled as pseudo-steady state plug flow reactors.

Table 1. Lumping of TMP Reaction System

symbol	lump name	boiling range
A	Heavy oil (HCO)	350-500℃
B	Diesel	204-350℃
	Gasoline	-
C	Alkenes	C_5-204℃
D	Aromatics	C_5-204℃
E	Paraffins+Naphthenes	C_5-204℃
	Liquid petroleum gas	-
F	Butane+Propane	$C_4^0+C_3^0$
G	Butene	$C_4^=$
H	Propylene	$C_3^=$
	Dry gas	-
I	Ethylene	$C_2^=$
J	Ethane+Methane+Hydrogen	$C_2^0+C_1+H_2$
K	Coke	-

The reaction rate of lump *i* towards lump *j*, $r_{i\to j}$, is given by

$$r_{i\to j}=\Phi_d k_{0,i\to j}\exp\left(-\frac{E_{i\to j}}{RT_{\text{ris}}}\right)y_i^{n_{i\to j}},\ i,j=A,B,\cdots,K \tag{1}$$

The deactivation function Φ_d is expressed as

$$\Phi_d=\frac{1}{1+\dfrac{3.68N}{100R_{\text{C/O}}}}\frac{1}{1+\dfrac{2.10A_h}{100R_{\text{C/O}}}}\left(1+14.36\frac{y_K}{R_{\text{C/O}}}\right)^{-0.20} \tag{2}$$

Where the values of deactivation constants N and A_h are 0.1 and 22.64, respectively (data from Daqing atmospheric residue), $R_{\text{C/O}}$ denotes the catalyst-to-oil weight ratio and y_{K} represents the mass fraction of coke in the 11lumps. In two risers, the mass fraction for each lump y_i can be expressed as in dimensionless form for $Z\in(0,1)$.

$$\begin{cases}\dfrac{\mathrm{d}y_{i,1}}{\mathrm{d}Z}=\dfrac{A_{\text{ris},1}L_{\text{ris},1}\rho_{\text{v},1}\varepsilon_{\text{ris},1}}{F_{\text{oil}}}\left(\sum_j r_{j\to i,1}-\sum_j r_{i\to j,1}\right)\\[2ex] \dfrac{\mathrm{d}y_{i,2}}{\mathrm{d}Z}=\dfrac{A_{\text{ris},2}L_{\text{ris},2}\rho_{\text{v},2}\varepsilon_{\text{ris},2}}{F_{\text{HCO}}+F_{\text{gasoline}}}\left(\sum_j r_{j\to i,2}-\sum_j r_{i\to j,2}\right)\end{cases} \tag{3}$$

Reaction temperatures along two risers follow the energy balance and thus can be expressed by

$$\begin{cases}\dfrac{\mathrm{d}T_{\text{ris},1}}{\mathrm{d}Z}=\dfrac{A_{\text{ris},1}L_{\text{ris},1}\rho_{\text{v},1}\varepsilon_{\text{ris},1}\left(\sum_j r_{j\to i,1}\Delta Hr_{j\to i}-\sum_j r_{i\to j,1}\Delta Hr_{i\to j}\right)}{\left(F_{\text{oil}}Cp_{\text{v},1}+G_{\text{reg},1}Cp_{\text{cat}}\right)}\\[3ex] \dfrac{\mathrm{d}T_{\text{ris},2}}{\mathrm{d}Z}=\dfrac{A_{\text{ris},2}L_{\text{ris},2}\rho_{\text{v},2}\varepsilon_{\text{ris},2}\left(\sum_j r_{j\to i,2}\Delta Hr_{j\to i}-\sum_j r_{i\to j,2}\Delta Hr_{i\to j}\right)}{\left(\left(F_{\text{HCO}}+F_{\text{gasoline}}\right)Cp_{\text{v},2}+G_{\text{reg},2}Cp_{\text{cat}}\right)}\end{cases} \tag{4}$$

The high-efficient feed injection system allows the feedstock to be completely and instantaneously vaporized with hot regenerated catalyst at the bottom of each riser. Boundary conditions, at Z=0, for Equations (4), can be obtained by a stationary energy balance around the mixer of the regenerated catalyst, lift/atomizing steam, and feedstocks.

Mass balances for the catalyst inventory, the coke content along with the energy balance of the stripper are described by Equation (5).

$$\begin{cases} \dot{W}_{\mathrm{st}} = G_{\mathrm{sp},1} + G_{\mathrm{sp},2} - G_{\mathrm{sp}} \\ W_{\mathrm{st}}\dot{C}_{\mathrm{sp}} = G_{\mathrm{sp},1}\left(C_{\mathrm{ris},1} - C_{\mathrm{sp}}\right) + G_{\mathrm{sp},2}\left(C_{\mathrm{ris},2} - C_{\mathrm{sp}}\right) \\ W_{\mathrm{st}}\dot{T}_{\mathrm{sp}} = G_{\mathrm{sp},1}\left(T_{\mathrm{ris},1}|_{Z=1} - T_{\mathrm{sp}}\right) + G_{\mathrm{sp},2}\left(T_{\mathrm{ris},2}|_{Z=1} - T_{\mathrm{sp}}\right) \end{cases} \tag{5}$$

The regenerator system can be modelled as two continuous stirred-tank reactors (CSTRs) in series. Specifically, the high-efficiency combustor and the dense region of the fluidized bed reactor are modelled as CSTRs. These two parts are connected by internal circulated catalyst. Effects of the freeboard region on the overall performance are ignored. Mass balances for catalyst inventory, carbon, hydrogen, and oxygen content along with the energy balance of the combustor are shown by Equation (6)-(10).

$$\dot{W}_{\mathrm{rg1}} = G_{\mathrm{sp}} + G_{\mathrm{rg21}} - G_{\mathrm{rg1}} \tag{6}$$

$$\dot{C}_{\mathrm{rg1}} = \frac{\left(G_{\mathrm{sp}} + G_{\mathrm{rg21}}\right)\left(C_{\mathrm{rg0}} - C_{\mathrm{rg1}}\right)}{W_{\mathrm{rg1}}} - k_{0,\mathrm{C}} \exp\left(\frac{E_{\mathrm{C}}}{RT_{\mathrm{rg1}}}\right) C_{\mathrm{rg1}} P_{\mathrm{rg1}} y_{\mathrm{O_2,rg1}} \tag{7}$$

$$\dot{H}_{\mathrm{rg1}} = \frac{\left(G_{\mathrm{sp}} + G_{\mathrm{rg21}}\right)\left(H_{\mathrm{rg0}} - H_{\mathrm{rg1}}\right)}{W_{\mathrm{rg1}}} - k_{0,\mathrm{H}} \exp\left(\frac{E_{\mathrm{H}}}{RT_{\mathrm{rg1}}}\right) H_{\mathrm{rg1}} P_{\mathrm{rg1}} y_{\mathrm{O_2,rg1}} \tag{8}$$

$$F_g\left(y_{\mathrm{O_2,rg0}} - y_{\mathrm{O_2,rg1}}\right) = \left(G_{\mathrm{sp}} + G_{\mathrm{rg21}}\right)\left(\frac{\left(C_{\mathrm{rg0}} - C_{\mathrm{rg1}}\right)}{12} + \frac{\left(H_{\mathrm{rg0}} - H_{\mathrm{rg1}}\right)}{4}\right) \tag{9}$$

$$\dot{T}_{\mathrm{rg1}} = \frac{\rho_{\mathrm{cat}}(1-\varepsilon_{\mathrm{rg1}})}{W_{\mathrm{rg1}}\left(\rho_{\mathrm{cat}}(1-\varepsilon_{\mathrm{rg1}})Cp_{\mathrm{cat}} + \rho_{\mathrm{g}}\varepsilon_{\mathrm{rg1}}Cp_{\mathrm{g}}\right)} \left(\begin{array}{l} \left(G_{\mathrm{sp}} + G_{\mathrm{rg21}}\right)Cp_{\mathrm{cat}}\left(T_{\mathrm{rg0}} - T_{\mathrm{rg1}}\right) + F_{\mathrm{g}}Cp_{\mathrm{g}}\left(T_{\mathrm{in,g}} - T_{\mathrm{rg1}}\right) \\ + \left(\begin{array}{l} k_{0,\mathrm{C}} \exp\left(\frac{E_{\mathrm{C}}}{RT_{\mathrm{rg1}}}\right) C_{\mathrm{rg1}}\left(-\Delta H_{\mathrm{C}}\right) + \\ k_{0,\mathrm{H}} \exp\left(\frac{E_{\mathrm{H}}}{RT_{\mathrm{rg1}}}\right) H_{\mathrm{rg1}}\left(-\Delta H_{\mathrm{H}}\right) \end{array}\right) P_{\mathrm{rg1}} y_{\mathrm{O_2,rg1}} W_{\mathrm{rg1}} \end{array}\right) \tag{10}$$

Mass balances for catalyst inventory, carbon and oxygen along with the energy balance of the dense region of the fluidized bed reactor are described by Equation (11)-(14).

$$\dot{W}_{\mathrm{rg2}} = G_{\mathrm{rg1}} - G_{\mathrm{rg2}} - G_{\mathrm{rg21}} \tag{11}$$

$$\dot{C}_{\mathrm{rg2}} = \frac{G_{\mathrm{rg1}}\left(C_{\mathrm{rg1}} - C_{\mathrm{rg2}}\right)}{W_{\mathrm{rg2}}} - k_{0,\mathrm{C}} \exp\left(\frac{E_{\mathrm{C}}}{RT_{\mathrm{rg2}}}\right) C_{\mathrm{rg2}} P_{\mathrm{rg2}} y_{\mathrm{O_2,rg2}} \tag{12}$$

$$F_{\mathrm{g}}\left(y_{\mathrm{O_2,rg1}} - y_{\mathrm{O_2,rg2}}\right) = G_{\mathrm{rg1}}\left(C_{\mathrm{rg1}} - C_{\mathrm{rg2}}\right)/12 \tag{13}$$

$$\dot{T}_{\mathrm{rg2}} = \frac{\rho_{\mathrm{cat}}(1-\varepsilon_{\mathrm{rg2}})}{W_{\mathrm{rg2}}\left(\rho_{\mathrm{cat}}(1-\varepsilon_{\mathrm{rg2}})Cp_{\mathrm{cat}} + \rho_{\mathrm{g}}\varepsilon_{\mathrm{rg2}}Cp_{\mathrm{g}}\right)} \times \left(\begin{array}{l} G_{\mathrm{rg1}}Cp_{\mathrm{cat}}\left(T_{\mathrm{rg1}} - T_{\mathrm{rg2}}\right) + F_{\mathrm{g}}Cp_{\mathrm{g}}\left(T_{\mathrm{rg1}} - T_{\mathrm{rg2}}\right) + \xi A_{\mathrm{tr}}\left(T_{\mathrm{cw}} - T_{\mathrm{rg2}}\right) \\ + k_{0,\mathrm{C}} \exp\left(\frac{E_{\mathrm{C}}}{RT_{\mathrm{rg2}}}\right) C_{\mathrm{rg2}} P_{\mathrm{rg2}} y_{\mathrm{O_2,rg2}}\left(-\Delta H_{\mathrm{C}}\right) W_{\mathrm{rg2}} \end{array}\right) \tag{14}$$

Validations of the model have been conducted under steady-state conditions using experimental data sets collected from a pilot-scale riser-regenerator system (Gan *et al*. 2011).

4. OPERABILITY ANALYSIS

Input/output multiplicity as a complex phenomenon that could be encountered in chemical processes may adversely affect the control performance. To design a reliable control framework for the TMP process, a comprehensive elucidation of the steady state multiplicity behaviour and a detailed knowledge of the corresponding (un)stable characteristic are prerequisites. Fig.2 discloses behaviour of main output variables as functions of catalyst circulation rate to the first riser, $G_{\mathrm{reg},1}$. Four sub-figures illustrate behaviours of outlet temperature of regenerator, T_{rg2}, oxygen content of flue gas, y_{O2}, and temperatures at the output of two risers ($T_{\mathrm{ris},1|Z=1}$ and $T_{\mathrm{ris},2|Z=1}$), respectively. When $G_{\mathrm{reg},1}$ is selected as the manipulated variable, there is a maximum and minimum $G_{\mathrm{reg},1}$ above and below which there is only a trivial steady state. Within a sufficient wide range, output multiplicity and input multiplicity will simultaneously appear.

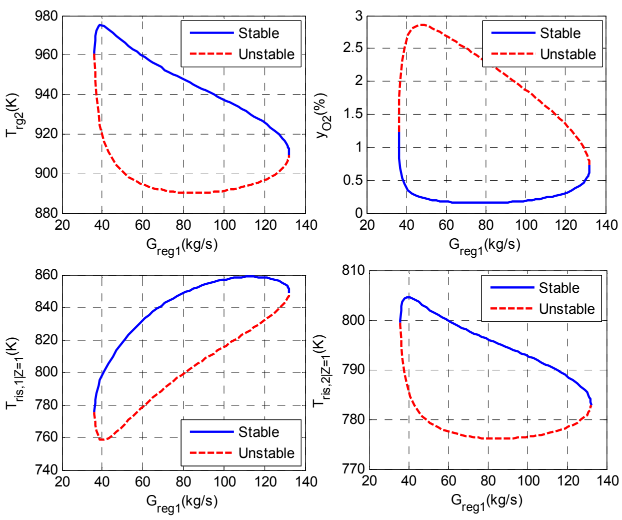

Fig.2. Steady state behaviours of TMP process under the nominal operating condition reported by (Li *et al*. 2007). (Solid lines refer to stable branches of the steady-state whereas dotted lines denote unstable branches)

From Fig.2, it can be seen that T_{rg2} and $T_{\mathrm{ris},2|Z=1}$ reach their own maximum simultaneously with increases in $G_{\mathrm{reg},1}$. The opposite holds for y_{O2} which crosses through its minimum value and then increases. However, for achieving the maximum value of $T_{\text{ris},1|Z=1}$, additional increase in $G_{\text{reg},1}$ is required. Within the operating region of $G_{\text{reg},1}$, all upper temperatures are stable which can be determined through heat generation/removal analysis of the regenerator system. On the other hand, a phenomenon typically associated with systems exhibiting input multiplicities is the change in the sign of the steady-state gain in the operating region. A smooth change in the sign of the steady-state gain implies that the steady state gain reduces to zero at some singular points in the operating region. As a result, the robustness of the linear controller with integral action is lost in the presence of input multiplicity (Morari, 1983). For example, the value of $T_{\text{ris},1|Z=1}$ with 780K corresponds to two values of $G_{\text{reg},1}$, one of which is obviously stable and another is unstable. Without an appropriate control system, the TMP process may switch from stable mode to unstable mode and simultaneously move temperatures of the regenerator and the second riser toward their lower values (Yuan *et al.* 2015).

5. EMPC FOR MAXIMUM PROPYLENE PRODUCTION

5.1 Recursive state estimation

In this work, the reaction heat of heavy oil, ΔHr_{A}, and the reaction heat of gasoline $\Delta Hr_{\text{gasoline}}$, which reflect the impact of feed properties variations on product distribution significantly, are chosen to be augmented as state variables

$$\dot{\boldsymbol{p}} = 0 \,,\, \boldsymbol{p}(t_0) = \boldsymbol{p}_0 \tag{15}$$

where $\boldsymbol{p} = [\Delta Hr_{\text{A}}, \Delta Hr_{\text{gasoline}}]^{\text{T}}$. The resulting augmented model of TMP process can now be represented in an abstract form by the semi-explicit DAE system

$$\boldsymbol{x}_{k+1} = \boldsymbol{x}_k + \int_{(k)\Delta t}^{(k+1)\Delta t} \boldsymbol{f}\left(\boldsymbol{x}(t), \boldsymbol{z}(t), \boldsymbol{u}(t)\right) dt + \boldsymbol{w}_{k+1} \tag{16}$$

$$\boldsymbol{g}\left(\boldsymbol{x}(t), \boldsymbol{z}(t), \boldsymbol{u}(t)\right) = 0, k\Delta t \le t \le (k+1)\Delta t \tag{17}$$

$$\boldsymbol{y}_{k+1} = \boldsymbol{h}\left(\boldsymbol{x}_{k+1}, \boldsymbol{z}_{k+1}\right) + \boldsymbol{v}_{k+1} \tag{18}$$

where $\boldsymbol{x}_{k+1} \in R^n$ and $\boldsymbol{z}_{k+1} \in R^{n_z}$ are the augmented differential states and the algebraic states at time $t = (k+1)\Delta t$, respectively, $\boldsymbol{w}_{k+1} \in R^{n_x}$ and $\boldsymbol{v}_{k+1} \in R^{n_y}$ are assumed to be independent Gaussian white noise processes with the covariance matrix $\boldsymbol{Q}_{k+1}$ and $\boldsymbol{R}_{k+1}$, respectively. Given Equations (1)-(14), the modified unscented Kalman filter (UKF) algorithm presented by (Mandela et al. 2010) is employed here to estimate these unmeasured state and model parameters from the available measurements. A salient feature of the UKF formulation is that it can utilize measurements of both algebraic and differential states. This feature is particularly useful since the measured temperatures at the output of two risers ($T_{\text{ris},1|Z=1}$ and $T_{\text{ris},2|Z=1}$) as well as the oxygen content of flue gas (y_{O2}) are treated as algebraic states, whereas T_{rg2} is treated as differential state.

5.2 Economics-oriented controller

An economics-oriented NMPC formulation for maximizing propylene production is given as follows:

$$\max_{\boldsymbol{u}} J = \int_{t_0}^{t_f} \left(w_1 F_{\text{oil}} y_{\text{H},1|Z=1} + w_2 \left(F_{\text{HCO}} + F_{\text{gasoline}} \right) y_{\text{H},2|Z=1} + \dot{\boldsymbol{u}} \boldsymbol{R} \dot{\boldsymbol{u}}^{\text{T}} \right) dt \tag{23}$$

Subject to

Equations (1)-(7)

$$\underline{\boldsymbol{u}} \le \boldsymbol{u} \le \overline{\boldsymbol{u}} \,,\, \underline{\dot{\boldsymbol{u}}} \le \dot{\boldsymbol{u}} \le \overline{\dot{\boldsymbol{u}}} \tag{24}$$

$$\underline{T}_{\text{rg},2} \le T_{\text{rg},2} \le \overline{T}_{\text{rg},2} \,,\, \underline{y}_{\text{O}_2} \le y_{\text{O}_2} \le \overline{y}_{\text{O}_2} \tag{25}$$

$$\underline{T}_{\text{ris},1|Z=1} \le T_{\text{ris},1|Z=1} \le \overline{T}_{\text{ris},1|Z=1} \,,\, \underline{T}_{\text{ris},2|Z=1} \le T_{\text{ris},2|Z=1} \le \overline{T}_{\text{ris},2|Z=1} \tag{26}$$

$$\frac{\int_{t_0}^{t_f} y_{\text{A},1|Z=1} dt}{t_f} \ge \underline{y}_{\text{A},1|Z=1} \tag{27}$$

$$\frac{\int_{t_0}^{t_f} \left(y_{\text{C},1|Z=1} + y_{\text{D},1|Z=1} + y_{\text{E},1Z=1} \right) dt}{t_f} \ge \underline{y}_{\text{Gasoline},1|Z=1} \tag{28}$$

$$\frac{\int_{t_0}^{t_f} \left(y_{\text{C},2|Z=1} + y_{\text{D},2|Z=1} + y_{\text{E},2|Z=1} \right) dt}{t_f} \ge \underline{y}_{\text{Gasoline},2|Z=1} \tag{29}$$

where $W = [w_1, w_2]$ are the constant weighting coefficients which are chosen such that each term in the objective function is significant, $\boldsymbol{u} = [G_{\text{reg},1}, G_{\text{reg},2}, F_c]^{\text{T}}$ are manipulated variables, $y_{\text{H},1,2|Z=1}$, $y_{\text{A},1|Z=1}$,and $\underline{y}_{\text{Gasoline},1,2|Z=1}$ are the estimated yields of propylene, feedstock, gasoline at the output of two risers, respectively. Equations (27)-(28) are used to constraint the heavy oil conversion and the gasoline yield in the first riser, respectively, so that there will be sufficient feedstock for the second riser. Equation (29) guarantees that the high-quality gasoline produced by the second riser is able to meet market demands.

The pseudospectral method (Garg *et al.* 2010) is used to transfer the original continuous dynamic optimization problem into a discrete nonlinear programming problem (NLP) by approximating the state and control profiles by a family of polynomials on finite elements. The resulting NLP is then solved using the efficient interior point-based large-scale nonlinear optimization algorithm (IPOPT, Wächter & Biegler, 2006)). At each execution cycle, IPOPT is initialized with a warm start constructed from the previous solution to make the solver converge faster.

6. SIMULATION

It was assumed that the flowrate of fresh feedstock to the first riser was fixed at $F_{\text{oil}} = 15\text{t/h}$, while the flowrate of recycling oil and crude gasoline to the second riser were equal to those produced by the first riser. Two scenarios have been considered: In scenario A, the TMP process was initially operated at the operating point reported by Li *et al.* 2007, the controller aimed at seeking optimal operating condition while satisfying its limitations and product specifications. In scenario B, The robustness of the control system was examined with respect to noise and uncertainties which were realized by varying key parameters of the process. The constraints and the tuning parameters used in NMPC formulations were listed in Table 2 and Table 3, respectively.

Table 2. Constraints to the TMP Process

constraint	unit	constraint	unit
$30 \le G_{\mathrm{reg},1} \le 56$	kg/s	$-0.2 \le \dot{G}_{\mathrm{reg},1} \le 0.2$	kg/s
$18 \le G_{\mathrm{reg},2} \le 36$	kg/s	$-0.2 \le \dot{G}_{\mathrm{reg},2} \le 0.2$	kg/s
$0 \le F_c \le 10$	kg/s	$-0.4 \le \dot{F}_c \le 0.4$	kg/s
$480 \le T_{\mathrm{ris},1\vert Z=1} \le 540$	K	$490 \le T_{\mathrm{ris},2\vert Z=1} \le 550$	K
$680 \le T_{\mathrm{rg},2} \le 740$	K	$0 \le y_{\mathrm{O}_2} \le 3$	%
$\underline{y}_{\mathrm{A},1\vert Z=1} = 15$	%	$\underline{y}_{\mathrm{Gasoline},1\vert Z=1} = 25$	%
$\underline{y}_{\mathrm{Gasoline},2\vert Z=1} = 35$	%		

Table 3. NMPC Tuning Parameters

parameter	value
sampling time, t_s	3s
prediction horizon, t_f	60s
control horizon, t_c	6s
weighting matrix, $\boldsymbol{W}$	$[10^3, 10^3]$
weighting matrix, $\boldsymbol{R}$	[10,10,1]

6.1 *Simulation of nominal operation scenarios*

A simulation run for maximizing propylene production from the experimental point has been conducted. Profiles of process outputs $T_{\mathrm{ris},1|Z=1}$, $T_{\mathrm{ris},2|Z=1}$, $T_{\mathrm{rg}2}$, and the corresponding manipulated inputs $G_{\mathrm{reg},1}$, $G_{\mathrm{reg},1}$, F_{c} in the presence of measurement noise are presented in Fig.3. The transients of feed conversion of the first riser, $y_{\mathrm{A},1|Z=1}$, gasoline yield of the second riser, $y_{\mathrm{Gasoline},2|Z=1}$, and propylene yields of the two risers $y_{\mathrm{H},1|Z=1}$, $y_{\mathrm{H},2|Z=1}$ are shown in Fig.4.

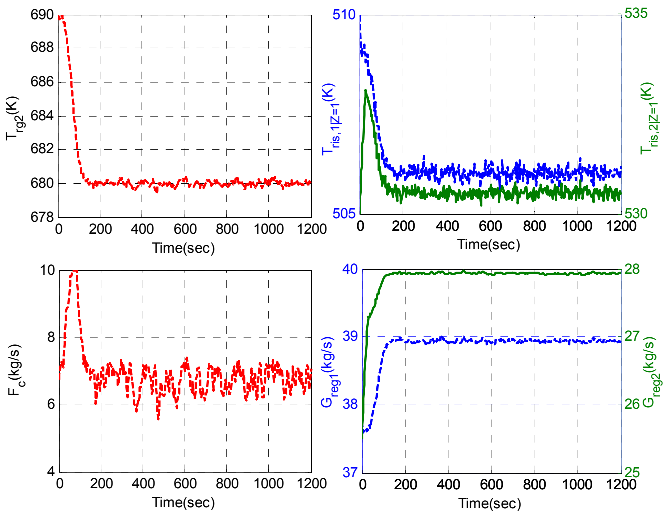

Fig.3. Profiles of the process outputs and the manipulated inputs for maximizing propylene production.

Initially, the TMP unit is operated under a sub-optimal condition where the propylene yields of the two risers are $y_{\mathrm{H},1|Z=1}$=16.9%, $y_{\mathrm{H},2|Z=1}$=15.4%, respectively. After turning on the controller, the cooling water flowrate, F_{c}, is adjusted so that the regenerator temperature, $T_{\mathrm{rg}2}$, rapidly decreases and finally remains around its lower limit. The reduction of the regenerator temperature lowers the contacting temperature at the mixing instant of the regenerated catalyst and oil vapor and thus requires increasing catalyst circulation rates to the two risers to maintain heat balance between the riser-regenerator system. On the basis of the fact that increasing the CTO without raising the reaction temperature can enhance catalytic pyrolysis reaction and minimize thermal cracking, $y_{\mathrm{H},1|Z=1}$ and $y_{\mathrm{H},2|Z=1}$ will keep increase until the constraints on $y_{\mathrm{A},1|Z=1}$ and $y_{\mathrm{Gasoline},2|Z=1}$ become active , and finally stabilize at the point with $y_{\mathrm{H},1|Z=1}$=17.2%, $y_{\mathrm{H},2|Z=1}$=16.2%, respectively. Simulation results show that the controller is capable of driving the process very close to its operational limits and exploiting the full economic potential for maximizing propylene production.

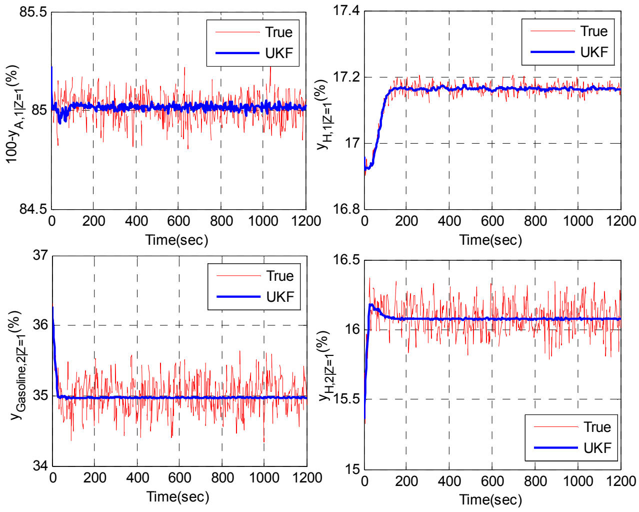

Fig.4. Profiles of the process constraints and propylene yields of the two risers.

6.2 *Robustness analysis*

To illustrate the robustness of the controller, simulations with plant-model mismatch are presented here. It is assumed that the TMP process is initially operated at the optimal operating point obtained in the previous section, model errors are then introduced by changing two key model parameters, ΔHr_{A} and $\Delta Hr_{\mathrm{gasoline}}$, by -10% and -20% (compared to the associated nominal ones) simultaneously at t=300s and by +10% and +20% (compared to the associated nominal ones) simultaneously at t=1500s, respectively. Fig.5 illustrates the output/input responses for the assumed plant-model mismatch and Fig.6 depicts the corresponding evolution of product yields at the output of two risers.

As can be seen from Fig.5 and Fig.6, when ΔHr_{A} and $\Delta Hr_{\mathrm{gasoline}}$ decrease at t=300s, both the heavy oil in the first riser and the gasoline in the second riser turn to be easily cracked, leading to increases of the feed conversion and the coke yield in the two risers. At this point, $y_{\mathrm{A},1|Z=1}$ and $y_{\mathrm{Gasoline},2|Z=1}$ begin to violate their respective lower bounds, require the controller reducing $G_{\mathrm{reg},1}$and $G_{\mathrm{reg},1}$ until the constraints are satisfied. Meanwhile, F_{c} increases to control $T_{\mathrm{rg}2}$ around its lower bound, avoiding $G_{\mathrm{reg},1}$ and $G_{\mathrm{reg},1}$ reduced too much, which is unfavourable for maximizing propylene yield. Here, an interesting phenomenon can be found, the decrease of ΔHr_{A} will initially lead to a sharp increase of

$y_{H,1|Z=1}$ which eventually reaches a new steady state lower than the initial value. In other words, an inverse response phenomenon exists, indicating input multiplicity between $G_{reg,1}$ and $y_{H,1|Z=1}$ may exist.

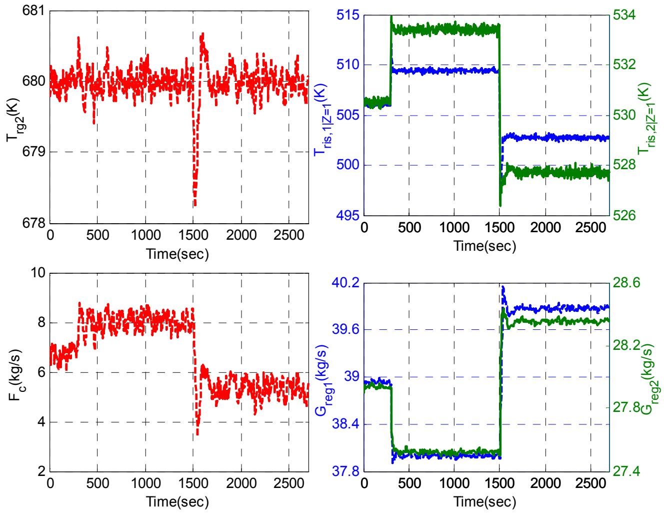

Fig.5. Profiles of the process outputs and the manipulated inputs under plant-model mismatch.

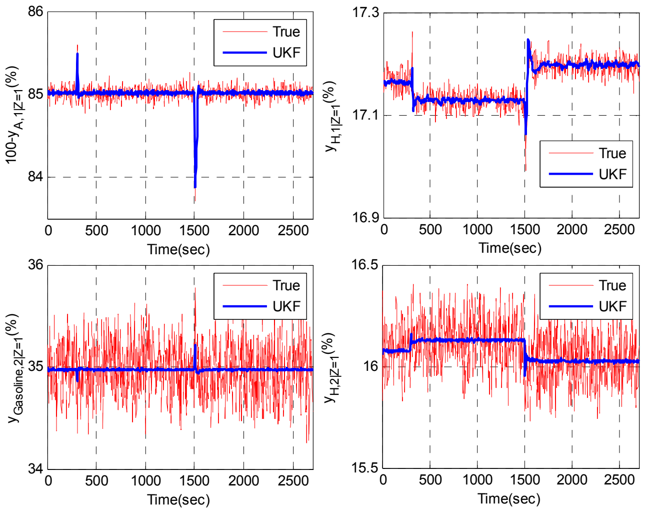

Fig.6. Profiles of process constraints and propylene yields of the two risers under plant-model mismatch.

Unlike the conventional set-point tracking controller, the economics-oriented tracking controller is inherently able to discriminate good and bad disturbances and exploit potential beneficial disturbances by continuously adapting the plant operating conditions to achieve economic optimisation. Specifically, in the presence of the economics-oriented tracking controller, a rise in $y_{H,1|Z=1}$ or $y_{H,2|Z=1}$ can be observed along with the increase of ΔHr_A or the decrease of $\Delta Hr_{gasoline}$, while respecting the constraints on $y_{A,1|Z=1}$ and $y_{Gasoline,2|Z=1}$.

7. CONCLUSIONS

An economics-oriented nonlinear MPC scheme was proposed for the optimization and control of the TMP process which exhibits complex nonlinear behavior. In order to tackle the barrier that the controlled variables cannot be measured online, an unscented transformation based Kalman filter was presented. The performance of the proposed controller was examined through seeking the optimal operation conditions to achieve the maximum propylene yield as well as desirable robustness against plant-model mismatches.

ACKNOWLEDGEMENT

The authors would like to gratefully acknowledge financial support from the Fundamental Research Funds for the Central Universities (Grant No. 13CX05021A and 15CX-02035A).

REFERENCES

Ellis, M., Durand, H., Christofides, P.D. (2014). A tutorial review of economic model predictive control methods. *Journal of Process Control*. 24(8):1156-1178.

Engell, S. (2007). Feedback control for optimal process operation. *Journal of Process Control*. 17: 203-219.

Gan, J.Q., Zhao, H., Berrouk, A.S., Yang, C.H., Shan, H.H. (2011). Numerical Simulation of Hydrodynamics and Cracking Reactions in the Feed Mixing Zone of a Multiregime Gas-Solid Riser Reactor. *Ind. Eng. Chem. Res*. 50 (20): 11511-11520.

Garg, D., Patterson, M. A., Hager, W. W., Rao, A. V., Benson, D. A., Huntington, G. T. (2010). A unified framework for the numerical solution of optimal control problems using pseudospectral methods. *Automatica*. 46, 1843-1851.

Guo, J. H. (2008). Primary Study of the Lumped Kinetic Model for Heavy Oil Cracking into Propylene by Two-Stage-Riser Technology. *M.S. Thesis*, China University of Petroleum, Dongying, China.

Li, C.Y., Yang, C.H., Shan, H.H. (2007). Maximizing propylene yield by two-stage riser catalytic cracking of heavy oil. *Ind. Eng. Chem. Res*. 46(14): 4914-4920.

Mandela, R. K., Rengaswamy, R., Narasimhan, S. (2010). Recursive state estimation techniques for nonlinear differential algebraic systems. *Chem. Eng. Sci*. 65:4548-4556.

Morari, M. (1983). Robust stability of systems with integral control. *In Proceedings of the 22nd IEEE Conference on Decision and Control*; IEEE Press: Piscataway, NJ. pp 865-869.

Qin, S.J., Badgwell, T.A. (2003). A survey of industrial model predictive control technology. *Control Engineering Practice*. 11(7): 733-764.

Shan, H.H., Dong, H.J., Zhang, J.F., Niu, G.L. (2001). Experimental study of two-stage riser FCC reactions. *Fuel*. 80(8): 1169-1175.

Wächter, A., Biegler, L. T. (2006). On the implementation of a primal-dual interior-point filter line-search algorithm for large-scale nonlinear programming. *Mathematical Programming*, 106(1): 25-57.

Yuan Z, Wang P, Yang C. (2015). Steady-state multiplicity analysis of two-stage-riser catalytic pyrolysis processes. *Computers & Chemical Engineering*, 73: 49-63.

Zanin, A. C., de Gouvea, M. T., Odloak, D. (2002). Integrating real-time optimization into the model predictive controller of the FCC system. *Control Engineering Practice*. 10, (8), 819-831.

